

Structural relaxation, softness and fragility of IPN Microgels

Valentina Nigro^{a,b,*}, Barbara Ruzicka^{a,b,**}, Beatrice Ruta^{c,d}, Federico Zontone^d, Monica Bertoldo^e, Elena Buratti^f, Roberta Angelini^{a,b},

^a*Istituto dei Sistemi Complessi del Consiglio Nazionale delle Ricerche (ISC-CNR), sede Sapienza, Pz.le Aldo Moro 5, I-00185 Roma, Italy*

^b*Dipartimento di Fisica, Sapienza Università di Roma, I-00185, Italy*

^c*CNRS Light Matter Institute, UMR5306, Lyon 1 University, Villeurbanne, France*

^d*ESRF The European Synchrotron, CS40220, 38043 Grenoble Cedex 9, France*

^e*Istituto per la Sintesi Organica e la Fotoreattività del Consiglio Nazionale delle Ricerche (ISOF-CNR), via P. Gobetti 101, 40129 Bologna, Italy*

^f*Istituto per i Processi Chimico-Fisici del Consiglio Nazionale delle Ricerche (IPCF-CNR), Area della Ricerca, Via G.Moruzzi 1, I-56124 Pisa, Italy*

Abstract

Soft colloids are elastic and deformable colloidal particles with a dual character somewhere between polymers and hard spheres. As a consequence of their hybrid nature soft colloids exhibit a larger variety of behaviours with respect to hard colloids still largely unexplored and able to provide new insight into the glass transition. Here the dynamics of a soft microgel made of interpenetrated polymer networks of PNIPAM and PAAc is investigated through X-ray Photon Correlation Spectroscopy and Dynamic Light Scattering. The existence of two dynamical regimes with increasing packing fraction is found, it is characterized by a crossover of the structural relaxation time at a critical concentration C_w^* from a super-Arrhenius growth to a slower than Arrhenius behaviour. This transition is also accompanied by a minimum of the β exponent in correspondence of C_w^* and by the existence of different diffusive regimes. A theoretical prediction to describe the experimental data is provided: at very low concentration the dynamics is well described by a Fickian diffusion, at intermediate concentrations an effective non Fickian anomalous diffusion has to be considered, while at the highest investigated concentrations the emergence of a ballistic motion is well described within the Mode Coupling Theory. Moreover the fragility of IPN microgels can be tuned by varying the particle softness thanks to the mutual PNIPAM-PAAc

*Corresponding author: valentina.nigro@uniroma1.it

**Corresponding author: barbara.ruzicka@roma1.infn.it

Corresponding author: roberta.angelini@roma1.infn.it

1. Introduction

In the last decades many works have been focused on the study of the glass transition in complex systems aiming at understanding differences and similarities between structural glasses (SG) and colloidal glasses (CG) [1–4]. In the case of structural glasses, as the liquid is rapidly quenched below its melting temperature, it undergoes a glass transition avoiding nucleation and crystallization. In colloids the transition is instead triggered by volume fraction ϕ or waiting time t_w (signaled by an aging phenomenon) whose increase drives the systems in an out-of-equilibrium configuration playing the role of $1/T$. Therefore changing control parameters like temperature, packing fraction or aging time, in both structural and colloidal glasses induces a slowing down of the dynamics yielding to a dramatic increase of the characteristic relaxation time ($\tau(T)$, $\tau(\Phi)$, $\tau(t_w)$) by several orders of magnitude up to reach a glassy state. The most direct way to access microscopic information on the relaxation dynamics is to look at the evolution of the intensity autocorrelation functions well described by the Kohlrausch-Williams-Watts (KWW) expression $F(Q,t) \propto \exp(-(t/\tau(Q))^\beta)$ where τ is an "effective" relaxation time and β measures the distribution of relaxation times (associated with simple exponential decays) and assumes generally positive values $\beta < 1$ (stretched behaviour). However recently an anomalous dynamics, characterized by a shape parameter $\beta > 1$ (compressed behaviour), has emerged in out of equilibrium states of different materials like colloidal glasses [5–13], gels [14–19], supercooled liquids [20, 21], metallic glasses [22, 23], polymeric systems [24–26], ceramics [27] and investigated also in theoretical [28–31] and simulation [32–35] works. The existence of stretched and/or compressed correlation functions is currently a very debated issue also faced in this work. Despite of many studies on the glass transition in SG and CG several questions are still open: Is the structural relaxation behaviour peculiar of the specific investigated system? How does it depend on the control parameters? What is the β parameter behaviour? What happens to the diffusive dynamics of the equilibrium liquid? In this paper, combining

X-ray Photon Correlation Spectroscopy (XPCS) and Dynamic Light Scattering (DLS), we answer these questions investigating the behaviour of the structural relaxation time and β exponent for a soft colloid. Soft colloids are an interesting class of glass-formers that, at variance with hard sphere-like colloids, provide a good tunability of particle softness giving rise to unconventional phase-behaviours [36–38]. They are indeed aqueous suspensions of nanometre- or micrometre-sized hydrogel particles sensitive to external stimuli whose dimension and effective volume fraction can be varied by changing external parameters such as temperature and/or pH.

The most studied responsive microgels are those based on the thermo-sensitive poly(*N*-isopropylacrylamide) (PNIPAM), with a reversible Volume Phase Transition (VPT) at about 305 K. It has been largely investigated both theoretically and experimentally [39–47]. In this work we will study a PNIPAM-based microgel with a second interpenetrated polymer network (IPN) of poly(acrylic acid) (PAAc) [48–56] that provides additional topological constraints to the particles and extra charges to the system. In this way the IPN microgel softness can be controlled by synthesis varying the amounts of poly(acrylic acid).

2. Experimental Methods

The dynamic structure factor has been investigated over a wide range of scattering vectors Q , correlation times t , weight concentrations C_w and PAAc content C_{PAAc} through combined XPCS and DLS techniques.

XPCS measurements were performed at the ID10 beamline at ESRF in Grenoble using a partially coherent x-ray beam with a photon energy of 21 keV. A series of scattering images were recorded by CdTe Maxipix detector (photon counting) and the ensemble averaged intensity autocorrelation function $g_2(Q, t) = \frac{\langle\langle I(Q, t_0)I(Q, t_0+t) \rangle\rangle_p}{\langle\langle I(Q, t_0) \rangle\rangle_p^2}$, where $\langle\langle \dots \rangle\rangle_p$ is the ensemble average over the detector pixels mapping onto a single Q value and $\langle \dots \rangle$ is the temporal average over t_0 , was calculated by using a standard multiple τ algorithm [57, 58]. XPCS data were complemented by DLS measurements performed at the CNR-ISC laboratory. The monochromatic and polarized beam emitted from a solid state laser (100 mW at $\lambda = 642$ nm) was focused on the sample placed in a cylindrical VAT for index matching and temperature control. The scattered intensity was simultaneously collected by single mode optical

fibers at five different scattering angles, namely $\theta=30^\circ, 50^\circ, 70^\circ, 90^\circ, 110^\circ$, corresponding to different scattering vectors Q , according to the relation $Q=(4\pi n/\lambda) \sin(\theta/2)$.

The investigated samples were IPN microgels synthesized by a sequential free radical polymerization method, then purified, lyophilized and diluted in water to the desired concentration under magnetic stirring for 1 day. A more detailed description of the preparation protocol is reported in Ref. [59, 60]. Samples at different concentrations were obtained by dilution at pH close to 5.5. The respective particle concentrations $\phi=nV_0$ were calculated from the number density $n=N_A\rho/M_w$ where N_A is the Avogadro number, ρ the density, M_w the molecular weight of the particles and $V_0 = \frac{4}{3}\pi R_0^3$ is the microgel particle volume at infinite dilution. Measurements were performed on aqueous suspensions of IPN microgels at five PAAc content ($C_{PAAc}=4\%$, $C_{PAAc}=9\%$, $C_{PAAc}=20\%$, $C_{PAAc}=23\%$, $C_{PAAc}=29\%$), fixed temperature above the VPTT ($T=311\text{ K}$), different particle concentrations in the range $C_w=(0.05 \div 5)\%$ and acidic pH (pH ~ 5.5) in the Q range $Q=(0.006 \div 0.063)\text{ nm}^{-1}$ below the peak of the static structure factor. The particles radius of the investigated samples at $T=311\text{ K}$ is: $C_{PAAc}=4\%$ $R=(26 \pm 3)\text{ nm}$, $C_{PAAc}=9\%$ $R=(56 \pm 4)\text{ nm}$, $C_{PAAc}=20\%$ $R=(68 \pm 3)\text{ nm}$, $C_{PAAc}=23\%$ $R=(103 \pm 4)\text{ nm}$, $C_{PAAc}=29\%$ $R=(130 \pm 2)\text{ nm}$. It increases with PAAc content as reported in [61].

3. Results and Discussion

Figure 1 shows DLS and XPCS intensity autocorrelation functions for IPN microgels with fixed PAAc content ($C_{PAAc}=29\%$) at different concentrations C_w and fixed temperature ($T=311\text{ K}$) when the particles are in the shrunken state. At low C_w values the intensity scattering functions are well described by a monomodal decay capturing the particle diffusion in the high dilution limit. As the particle concentration increases a dynamical decoupling is observed and a two-step relaxation, characteristic of glass-forming systems approaching the glass transition, comes out. The monomodal decay for $C_w \leq 0.6\%$ and the final decay for $C_w > 0.6\%$ are well described by the Kohlrausch-Williams-Watts expression [62]:

$$g_2(Q, t) = b[(A \exp(-(t/\tau(Q))^\beta))^2 + 1] \quad (1)$$

where $b \cdot A^2$ is the coherence factor, τ the structural relaxation time and β the shape

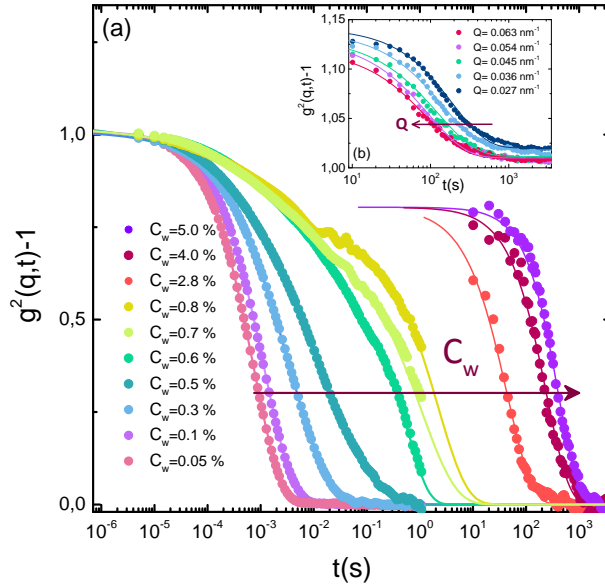


Figure 1 (a) Normalized intensity autocorrelation functions of IPN microgel particles containing 29 % of PAAc at $T=311$ K and $Q=0.022$ nm^{-1} as a function of concentration and (b) for a sample at $C_w=5.0$ % as a function of the scattering vector Q . The solid lines represent the best fits through Eq.(1).

exponent, representing a phenomenological hallmark of glass forming liquid dynamics. The fits are shown as full lines in Fig. 1.

The structural relaxation time τ is reported in Fig. 2(a). An interesting behaviour shows up: at low C_w τ grows exponentially up to a critical concentration value $C_w^* \sim 0.6$ % with a Vogel Fulcher Tamman (VFT) behaviour $\tau = \tau_0 \exp(\frac{D_c C_w}{C_{w0} - C_w})$ where C_w replaces $1/T$ and C_{w0} sets the apparent divergence. Above C_w^* it suddenly increases as a power law $\tau \sim C_w^\alpha$ with $\alpha = 2.6 \pm 0.1$ signing the existence of two different dynamical regimes. The relaxation time vs aging time t_w of an hard colloid, the largely studied Laponite[®] suspensions [6, 10, 64, 65], is reported in Fig. 2(b) from Ref. [8]. It changes from a VFT behaviour $\tau = \tau_0 \exp(\frac{D t_w}{t_w^\infty - t_w})$ [5, 7, 8, 12] where t_w replaces $1/T$ and t_w^∞ sets the apparent divergence [66, 67], to a slower than Arrhenius behaviour with increasing t_w . Moreover in Fig. 2(c) the temperature dependence of the structural relaxation time for a metallic glass from Ref. [23] is shown. Also in the case of metallic glasses, widely investigated in the last years [22, 23, 68], the existence of two dynamical regimes below and above the glass transition temperature T_g has been observed. After T_g the weaker temperature dependence of the structural relaxation time is well described, by an Arrhenius behaviour. It is worth to note

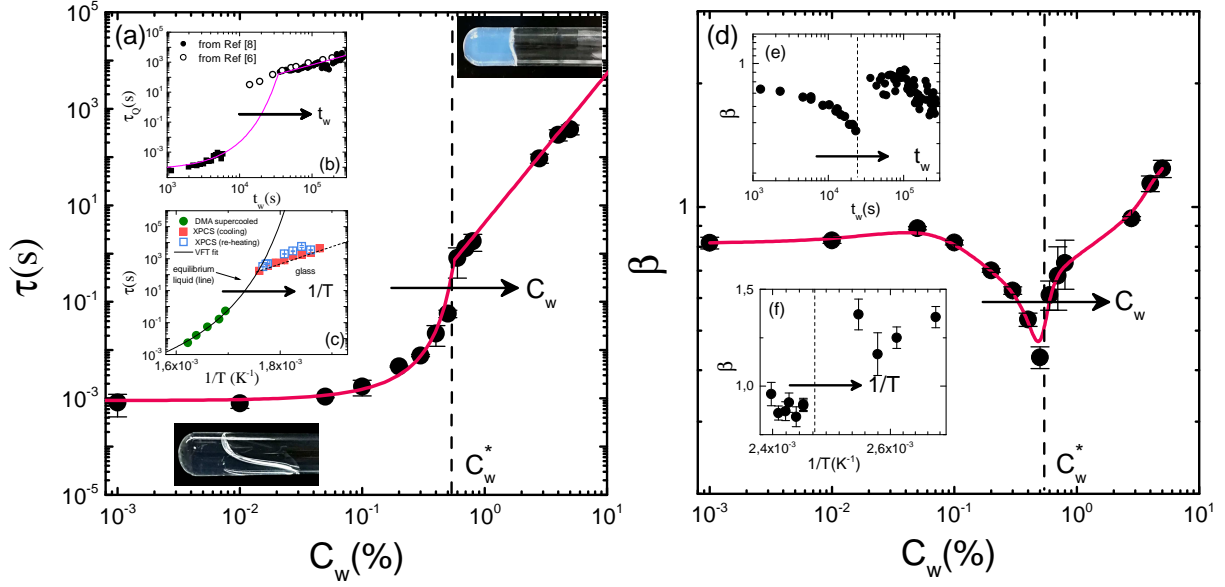


Figure 2 (a) Structural relaxation time from Eq.(1) as a function of weight concentration for IPN microgel suspensions containing 29 % of PAAc at $T=311$ K and $Q=0.022$ nm $^{-1}$. Full lines represent the best fits with VFT and power law behaviours at small and large C_w respectively. (b) Structural relaxation time behaviour with aging time t_w from Ref. [8] for colloidal suspensions of Laponite and (c) structural relaxation time behaviour with the inverse of temperature $1/T$ from Ref. [23] for a metallic glass. (d) β parameter from Eq.(1) as a function of weight concentration for IPN microgel suspensions. Full line is a guide to eyes. (e) β exponent as a function of aging time t_w from Ref. [8, 63] for colloidal suspensions of Laponite and (f) β exponent dependence with $1/T$ from Ref. [22] for a metallic glass.

that the dynamical crossover is reached by increasing concentration (Fig. 2(a)) or waiting time (Fig. 2(b)) in colloidal glasses and by decreasing temperature (Fig. 2(c)) in structural glasses. Our findings for IPN microgels suggest that a unifying scenario can be provided: the slowing down of the dynamics achieved by varying packing fraction [47, 69], waiting time [5, 7, 8, 12] or temperature [22, 23] is accompanied by a super Arrhenius increase, typically VFT, of the structural relaxation time followed by a slower than Arrhenius or an Arrhenius behaviour. Thus the existence of two different dynamical regimes is a general feature of soft colloids, hard colloids and structural glasses.

To complement these observations, we report in Fig. 2(d) the behaviour of the β parameter derived from the fits through Eq.(1). Surprisingly we find that the dynamical crossover at C_w^* is signaled by a sharp change of the shape parameter β from stretched ($\beta < 1$) to compressed ($\beta > 1$) in the high concentrated samples that we attribute to rising

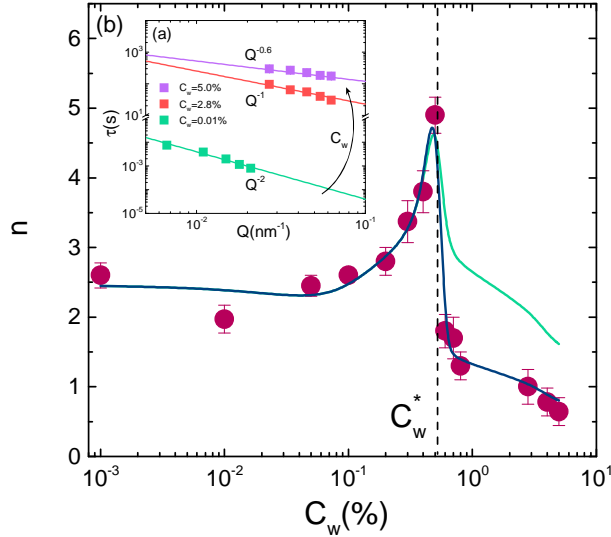


Figure 3 (a) Structural relaxation time as a function of the scattering vectors Q for IPN microgel suspensions containing 29 % of PAAc at $T=311$ K as measured through DLS and XPCS at increasing weight concentrations. Full lines represent the fits through Eq.2. (b) Power exponent from fits through Eq.2. Blue full line is the predicted behaviour from Eq.9 while green full line is the predicted behaviour using Eq.7 for all C_w .

stresses deriving from the high packaging of the particles. As in the case of the structural relaxation time, the behaviour of β is shown for the hard colloid of Ref. [8] as a function of t_w (Fig. 2(e)) and for the metallic glass of Ref. [23] as a function of $1/T$ (Fig. 2(f)). It is evident that for all these systems the dynamical crossover driven by C_w , t_w or T is always accompanied by a discontinuity of β , corroborating the existence of a universal behaviour regardless of the control parameter and the specific interactions of the system. It is worth to note that in the first dynamical regime β decreases below 1 while in the second one it increases to values up to $\simeq 1 \div 1.5$ depending on the system. This deviation from the common stretched behaviour can be attributed to the development of internal stresses at the transition [8, 14, 22]. The peculiar values of each system depend on the specific materials, on its history and/or on the preparation protocols whose optimization and control is subject of theoretical and experimental investigations.

The Q -dependence of the structural relaxation time for IPN microgel suspensions containing 29 % of PAAc at $T=311$ K in the Q range $Q=(0.006 \div 0.063)$ nm $^{-1}$ is reported in Fig. 3(a) at different concentrations. The data are well fitted through a power law

$$\tau(Q) \propto Q^{-n} \quad (2)$$

shown as solid lines in Fig. 3(a). The behaviour of n as a function of concentration is reported in Fig. 3(b). In the first dynamical regime, for low concentrations ($C_w \leq 0.1$ %) a quadratic wave vector dependence with $n \sim 2$ is found, this behaviour, typical of diffusive dynamics, is ruled out at increasing concentration where an increase of viscosity, observed by eyes, is accompanied by unusual values of n up to $n \sim 5$. In the second dynamical regime n suddenly decreases down to values $n \leq 1$ where the case of $n \sim 1$ is characteristic of the ballistic motion of particles. The crossover between the two dynamical regimes is characterized by a maximum in correspondence of the critical concentration value C_w^* and is also associated to the observed crossover of the structural relaxation time (Fig. 2(a)) and β parameter (Fig. 2(d)). Aiming to explain this behaviour we consider that at low concentrations ($C_w < 0.1$ %) the diffusion process is well described by Fickian diffusion, as the case of particles Brownian motion, and the mean square displacement $\langle r^2(t) \rangle$ has a time linear dependence according to:

$$\langle r^2(t) \rangle = 6Dt \quad (3)$$

where D is the particles diffusion coefficient. At increasing concentrations ($C_w > 0.1$ %) the system starts to become spatially heterogeneous, particles are no longer free to move as in the case of pure diffusive dynamics since they are trapped in cages characterised by different persisting times. In our experiments, since we are probing scattering vectors Q in the range $Q = (0.006 \div 0.063) \text{ nm}^{-1}$ that corresponds to length scales up to ten particles radii ($R = (103 \pm 4) \text{ nm}$), we are sensitive to these heterogeneities, with a resulting failure of Eq. 3 and the appearance of a non-Fickian anomalous diffusion [70] described by:

$$\langle r^2(t) \rangle = \Gamma t^\beta \quad (4)$$

with an effective diffusion coefficient [71, 72] $D(t) = \Gamma t^{\beta-1}$. The *diffusive dynamics* (Eq. 3) is recovered when $\beta = 1$ and $D(t) = \Gamma = 6D$. For $0 < \beta < 1$ the dynamics is *subdiffusive* and for $\beta > 1$ is *superdiffusive*, with the special case of $\beta = 2$ corresponding to *ballistic*

motion.

The mean square displacement, in the Gaussian approximation, is related to the intermediate scattering function as [62]:

$$F(Q,t) = \exp(-Q^2 \langle r^2(t) \rangle / 6) \quad (5)$$

that, using the generalized mean square displacement of Eq. 4, becomes $F(Q,t) = \exp(-\frac{Q^2\Gamma}{6}t^\beta)$. The comparison with the KWW expression of the intermediate scattering function $F(Q,t) \propto \exp(-(t/\tau(Q))^\beta)$, gives $(t/\tau(Q))^\beta = \frac{Q^2\Gamma}{6}t^\beta$ and:

$$(1/\tau(Q))^\beta = Q^2\Gamma/6 \quad (6)$$

that provides:

$$\tau(Q) \propto Q^{-2/\beta} \quad (7)$$

In the case of diffusive dynamics with $\beta=1$ one gets the typical $\tau(Q) \propto Q^{-2}$ behaviour while in the case of ballistic motion of particles with $\beta=2$ $\tau(Q) \propto Q^{-1}$. A comparison between Eq.2 and Eq.7 gives $n = 2/\beta$. This behaviour is reported in Fig.3(b) as green line. One can observe a good agreement with the experimental data only for $C_w < C_w^*$. The critical concentration C_w^* , characterized by a relaxation time of the order of seconds, sets the transition from a fluid to an intermediate state that is visually arrested, as shown in the top photograph of Fig.2. For $C_w \geq C_w^*$ the dynamics is progressively slowed down going towards a glassy state, as witnessed by the increasing relaxation times up to values of the order of thousand seconds. In this condition the Gaussian approximation of Eq.5 turns out to be increasingly inaccurate [73] and, in order to describe the dynamics approaching the glassy state, we refer to the Mode Coupling Theory (MCT) [74, 75] that provides a different Q -dependence of the structural relaxation time as:

$$\tau(Q) \propto Q^{-1/\beta} \quad (8)$$

Surprisingly for $C_w \geq C_w^*$ a perfect agreement is now observed as shown in Fig.3(b) (blue

full line). Therefore the experimental data are well described through:

$$\begin{aligned}\tau(Q) &\propto Q^{-2/\beta} & C_w < C_w^* \\ \tau(Q) &\propto Q^{-1/\beta} & C_w \geq C_w^*\end{aligned}\quad (9)$$

In order to understand the role of particles softness on the dynamics we report an Angell plot [76] of IPN microgels in Fig.4. More recently in fact the unifying concept of fragility has been extended to colloidal suspensions by replacing the inverse of temperature $1/T$ with concentration C_w [44, 45, 50, 77] and many efforts have been devoted to understand the effect of softness on fragility [50, 77–79]. To this aim we performed measurements on microgels as a function of particle softness by changing PAAc content. In particular in Fig.4(a) the normalised structural relaxation time at different PAAc content is reported as a function of packing fraction ϕ . One can observe two main features: the normalised structural relaxation time has a smoother and smoother packing fraction dependence with decreasing PAAc content and secondly a divergence occurs at lower packing fraction for particles with higher PAAc content. This can be related to the higher dimension (R increases from 56 nm to 130 nm) of particles and to the presence of increased interactions due to COOH groups belonging to PAAc chains as deeply discussed in [61]. Our data are well described by the VFT equation:

$$\tau = \tau_0 \exp\left(\frac{D_\phi \phi}{\phi_0 - \phi}\right) \quad (10)$$

where ϕ_0 sets the apparent divergence, D_ϕ controls the growth of the structural relaxation time on approaching ϕ^* and τ_0 is the characteristic structural relaxation time in the high dilution limit. This result points out that, as in the case of molecular glass formers [76], different dynamical behaviours can be achieved in microgels by changing PAAc content.

In order to obtain a renormalized Arrhenius plot we rescale ϕ by the packing fraction ϕ^* as shown in Fig.4(b). ϕ^* is defined as the packing fraction where the relaxation time is the same. At increasing PAAc content the curves depart more and more from the Arrhenius-

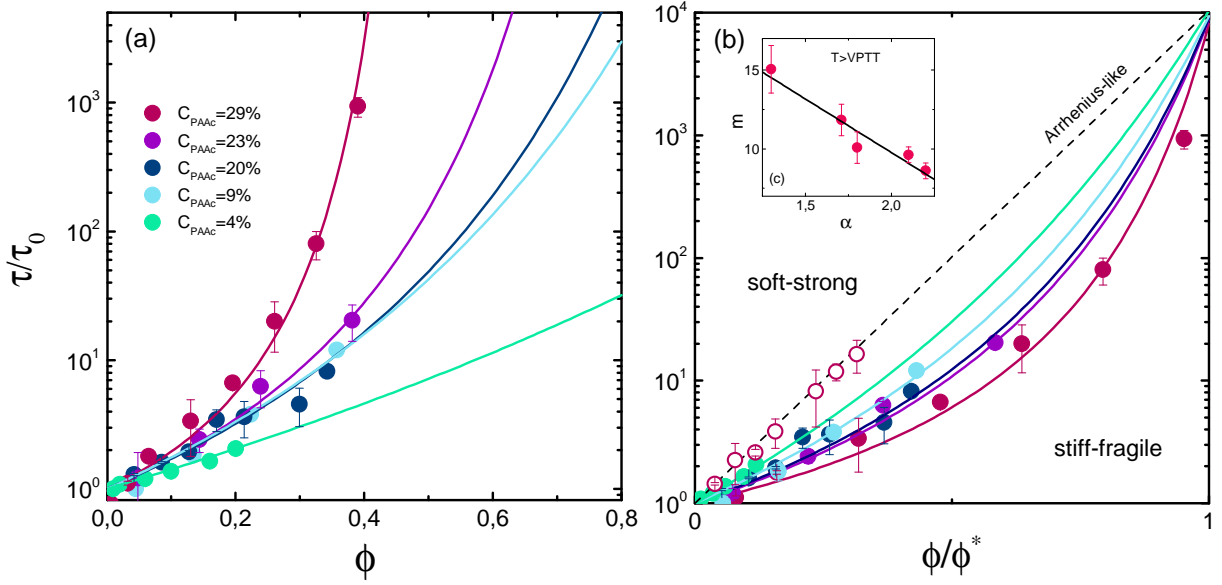


Figure 4 (a) Normalised structural relaxation time as a function of packing fraction at the indicated PAAc contents and $T=311$ K. Solid lines are fits through Eq.(10). (b) Angell plot for the normalised structural relaxation time versus normalised packing fraction at $T=311$ K (closed symbols) compared with data at $T=297$ K for a sample at 29 % of PAAc as an example (open symbols). Solid lines are fits according to the VFT equations using Eq.(1). (c) Fragility index m as a function of swelling ratio related to particles softness.

like behaviour that can be recovered only in the case of particles at room temperature in the completely shrunken state as shown in Fig.4(b) for the sample at 29 % of PAAc as an example (open symbols).

The slope of the data at $\phi = \phi^*$ defines the fragility as:

$$m = \left[\frac{\partial \log \tau}{\partial (\phi/\phi^*)} \right]_{\phi=\phi^*} \quad (11)$$

that is related to the particle softness provided by the swelling ratio defined as:

$$\alpha = \frac{R_H^{swollen}}{R_H^{shrunken}} \quad (12)$$

where $R_H^{swollen} = R(T=297 \text{ K})$ and $R_H^{shrunken} = R(T=311 \text{ K})$. Particles with higher softness can shrink more, providing an higher value of α . Interestingly it has been recently shown that α decreases with increasing PAAc content interpenetrated within the PNIPAM network

[61].

We can explore the role played by softness plotting the fragility m as a function of α (Fig.4(c)): it decreases with increasing softness in agreement with very recent theoretical results on the role of deformation in soft colloids [80]. Therefore the fragility of IPN microgels can be tuned by changing PAAc concentration. A clear picture of the relation between softness and fragility is thus provided: higher is the PAAc content stiffer are the particles, thus yielding to more fragile systems. This behaviour can be ascribed to the interpenetration of the second polymeric network that, introducing both additional topological constraints and extra charges, modulates the softness of the system.

4. Conclusions

In conclusion through XPCS and DLS measurements we have shown the existence of two dynamical regimes in PNIPAM-PAAc IPN microgels with a crossover of the structural relaxation time accompanied by a clear change of the β exponent from stretched ($\beta < 1$) to compressed ($\beta > 1$). The comparison with similar behaviours found in hard colloids and in metallic glasses indicates that these are general common features of different systems regardless of the control parameters (C_w , t_w , $1/T$) and of the specific interactions at stakes. The scattering vector dependence of the structural relaxation time in IPN microgels has shown a surprising behaviour of the derived power exponent with a maximum in correspondence of the dynamical crossover. We provide a theoretical prediction that well describes the experimental data: at very low concentration the dynamics is well described by a Fickian diffusion, at intermediate concentrations an effective non Fickian anomalous diffusion has to be considered, while at the highest investigated concentrations the emergence of a ballistic motion is well described within the Mode Coupling Theory. Moreover in IPN microgels an additional control parameter comes out: interpenetrating different amount of PAAc originates particles with varying softness allowing to modulate the fragility of the system. In particular the concentration dependence of the structural relaxation time can be easily controlled and the stiffest particles undergoes the dynamical crossover at the lowest particle concentration. This implies that increasing particle softness moves forward the critical packing fraction for the transition. All these findings add new insights to the so

far debated stretched to compressed transition and contribute to the further understanding of the role of softness in the fragility and to the analogies and differences between colloidal and structural glasses. In order to further test our findings and hypothesis, more experiments on a wide range of systems, will be useful.

Acknowledgments

The authors acknowledge acknowledge ESRF for beamtime and support from the European Research Council (ERC Consolidator Grant 681597, MIMIC) and from MIUR-PRIN (2012J8X57P).

Author contributions statement

R.A., V.N. and B.Ruz. conceived the experiments. R.A., V.N., B.R., B.Ruz. and F.Z. conducted the experiments. R.A., V.N. and B.Ruz. analysed the results. M.B. and E.B. synthesized the samples. R.A., V.N. and B.Ruz. wrote the manuscript.

References

- [1] F. Sciortino and P. Tartaglia, *Adv. Phys.*, 2005, **54**, 471–524.
- [2] V. Trappe and P. Sandkühler, *Curr. Opin. Colloid Interface Sci.*, 2004, **8**, 494–500.
- [3] W. C. K. Poon, *Curr. Opin. Colloid Interface Sci.*, 1998, **3**, 593–599.
- [4] E. Zaccarelli, *J. Phys.: Condens. Matter*, 2007, **19**, 323101–50.
- [5] M. Bellour, A. Knaebel, J. L. Harden, F. Lequeux and J. P. Munch, *Phys. Rev. E*, 2003, **67**, 031405–8.
- [6] R. Bandyopadhyay, D. Liang, H. Yardimci, D. A. Sessoms, M. A. Borthwick, S. G. J. Mochrie, J. L. Harden and R. L. Leheny, *Phys. Rev. Lett.*, **93**, 228302.
- [7] F. Schosseler, S. Kaloun, M. Skouri and J. P. Munch, *Phys. Rev. E*, **73**, 021401.
- [8] R. Angelini, L. Zulian, A. Fluerasu, A. Madsen, G. Ruocco and B. Ruzicka, *Soft Matter*, 2013, **9**, 10955–9.

- [9] R. Angelini, A. Madsen, A. Fluerasu, G. Ruocco and B. Ruzicka, *Colloids and Surfaces A: Physicochemical and Engineering Aspects*, 2014, **460**, 118–122.
- [10] R. Angelini, E. Zaccarelli, F. A. de Melo Marques, M. Sztucki, A. Fluerasu, G. Ruocco and B. Ruzicka, *Nat. Commun.*, 2014, **5**, 4049–7.
- [11] P. Kwaśniewski, A. Fluerasu and A. Madsen, *Soft Matter*, 2014, **10**, 8698–8704.
- [12] R. Angelini and B. Ruzicka, *Colloids and Surfaces A: Physicochemical and Engineering Aspects*, 2015, **483**, 316–320.
- [13] R. Pastore, G. Pesce and M. Caggioni, *Scientific Reports*, 2017, **7**, 43496–9.
- [14] L. Cipelletti, S. Manley, R. Ball and D. Weitz, *Phys. Rev. Lett.*, 2000, **84**, 2275–4.
- [15] B. Chung, S. Ramakrishnan, R. Bandyopadhyay, D. Liang, C. Zukoski, J. Harden and R. Leheny, *Phys. Rev. Lett.*, 2006, **96**, 228301–4.
- [16] H. Guo, S. Ramakrishnan, J. Harden and R. L. Leheny, *J. Chem. Phys.*, 2011, **135**, 154903–16.
- [17] D. Orsi, L. Cristofolini, G. Baldi and A. Madsen, *Phys. Rev. Lett.*, 2012, **108**, 105701–4.
- [18] L. Cristofolini, *Current Opinion in Colloid and Interface Science*, 2014, **19**, 228–241.
- [19] B. W. Mansel and M. A. K. Williams, *Soft Matter*, 2015, **11**, 7016–7023.
- [20] C. Caronna, Y. Chushkin, A. Madsen and A. Cupane, *Phys. Rev. Lett.*, 2008, **100**, 55702–4.
- [21] H. Conrad, F. Lehmkuhler, B. Fischer, F. Westermeier, M. A. Schroer, Y. Chushkin, C. Gutt, M. Sprung and G. Grübel, *Phys. Rev. E*, 2015, **91**, 042309–6.
- [22] B. Ruta, Y. Chushkin, G. Monaco, L. Cipelletti, E. Pineda, P. Bruna, V. Giordano and M. Gonzalez-Silveira, *Phys. Rev. Lett.*, 2012, **109**, 165701–4.
- [23] Z. Evenson, B. Ruta, S. Hechler, M. Stolpe, E. Pineda, I. Gallino and R. Busch, *Phys. Rev. Lett.*, 2015, **115**, 175701–4.

- [24] P. Falus, M. Borthwick, S. Narayanan, A. Sandy and S. Mochrie, *Phys. Rev. Lett.*, 2006, **97**, 066102–4.
- [25] R. A. Narayanan, P. Thiagarajan, S. Lewis, A. Bansal, L. S. Schadler and L. B. Lurio, *Phys. Rev. Lett.*, 2006, **97**, 075505–4.
- [26] S. Srivastava and A.K. Kandar and J.K. Basu and M.K. Mukhopathyay and L.B. Lurio and S. Narayanan and .K. Sinha, *Phys. Rev. E*, 2009, **79**, 021408–8.
- [27] V. Balitska, O. Shpotyuk, M. Brunner and I. Hadzaman, *Chemical Physics*, 2018, **501**, 121–127.
- [28] J. P. Bouchaud and E. Pitard, *The European Physical Journal E*, 2001, **6**, 231–236.
- [29] J. P. Bouchaud, *Anomalous Relaxation in Complex Systems: From Stretched to Compressed Exponentials*, 2008.
- [30] E. E. Ferrero, K. Martens and J.-L. Barrat, *Phys. Rev. Lett.*, 2014, **113**, 248301–4.
- [31] A. Nicolas, E. E. Ferrero, K. Martens and J.-L. Barrat, *arXiv:1708.09194v2*, 2018.
- [32] T. Morishita, *The Journal of Chemical Physics*, 2012, **137**, 024510–6.
- [33] M. Bouzid and J. Colombo and L. V. Barbosa and E. Del Gado, *Nat. Comm.*, 2017, **8**, 15846–8.
- [34] P. Chaudhuri and L. Berthier, *Phys. Rev. E*, 2017, **95**, 060601–6.
- [35] R. Pastore and G. Pesce and A. Sasso and M. Pica Ciamarra , *Colloids and Surfaces A: Physicochemical and Engineering Aspects*, 2017, **532**, 87–96.
- [36] C. N. Likos, *Phys. Rep.*, 2001, **348**, 267–439.
- [37] P. E. Ramírez-González and M. Medina-Noyola, *Journal of Physics: Condensed Matter*, 2009, **21**, 075101–13.
- [38] D. Vlassopoulos and M. Cloitre, *Current Opinion in Colloid & Interface Science*, 2014, **19**, 561–574.

- [39] R. H. Pelton, *Adv. Colloid Interface Sci.*, 2000, **85**, 1–33.
- [40] T. Hellweg, C. Dewhurst, E. Brückner, K. Kratz and W. Eimer, *Colloid. Polym. Sci.*, 2000, **278**, 972–978.
- [41] J. Wu, B. Zhou and Z. Hu, *Phys. Rev. Lett.*, 2003, **90**, 048304–4.
- [42] L. A. Lyon and A. Fernandez-Nieves, *Annu. Rev. Phys. Chem.*, 2012, **63**, 25–43.
- [43] D. Paloli, P. S. Mohanty, J. J. Crassous, E. Zaccarelli and P. Schurtenberger, *Soft Matter*, 2013, **9**, 3000–3004.
- [44] R. P. Seekell, P. S. Sarangapani, Z. Zhang and Y. Zhu, *Soft Matter*, 2015, **11**, 5485–5491.
- [45] S. K. Behera, D. Saha, P. Gadige and R. Bandyopadhyay, *Physical Review Materials*, 2017, **1**, 055603.
- [46] N. Gnan, L. Rovigatti, M. Bergman and E. Zaccarelli, *Macromolecules*, 2017, **50**, 8777.
- [47] A.-M. Philippe, D. Truzzolillo, J. Galvan-Myoshi, P. Dieudonné-George, V. Trappe, L. Berthier and L. Cipelletti, *Phys. Rev. E*, 2018, **97**, 040601.
- [48] X. Xia and Z. Hu, *Langmuir*, 2004, **20**, 2094–2098.
- [49] J. Zhou, G. Wang, L. Zou, L. Tang, M. Marquez and Z. Hu, *Biomacromolecules*, 2008, **9**, 142–148.
- [50] J. Mattsson, H. M. Wyss, A. Fernandez-Nieves, K. Miyazaki, Z. Hu, D. Reichman and D. A. Weitz, *Nature*, 2009, **462**, 83–86.
- [51] J. Ma, B. Fan, B. Liang and J. Xu, *J. Colloid Interface Sci.*, 2010, **341**, 88–93.
- [52] Z. Xing, C. Wang, J. Yan, L. Zhang, L. Li and L. Zha, *Colloid Polym. Sci.*, 2010, **288**, 1723–1729.
- [53] X. Liu, H. Guo and L. Zha, *Polymers*, 2012, **61**, 1144–1150.

- [54] Z. Li, J. Shen, H. Ma, X. Lu, M. Shi, N. Li and M. Ye, *Mater. Sci. Eng. C*, 2013, **33**, 1951–1957.
- [55] V. Nigro, R. Angelini, M. Bertoldo, V. Castelvetro, G. Ruocco and B. Ruzicka, *J. Non-Cryst. Solids*, 2015, **407**, 361–366.
- [56] V. Nigro, R. Angelini, M. Bertoldo, F. Bruni, M. Ricci and B. Ruzicka, *Soft Matter*, 2017, **13**, 5185–5193.
- [57] A. Madsen, R. Leheny, H. Guo, M. Sprung and O. Czakkel, *New J. of Phys.*, 2010, **12**, 055001–16.
- [58] R. L. Leheny, *Curr. Opin. Colloid Interface Sci.*, 2012, **17**, 3–12.
- [59] V. Nigro, R. Angelini, M. Bertoldo, F. Bruni, M. Ricci and B. Ruzicka, *J. Chem. Phys.*, 2015, **143**, 114904–9.
- [60] V. Nigro, R. Angelini, M. Bertoldo and B. Ruzicka, *Colloids Surf. A*, 2017, **532**, 389–396.
- [61] V. Nigro, R. Angelini, B. Rosi, M. Bertoldo, E. Buratti, S. Casciardi, S. Sennato and B. Ruzicka, *Submitted to Scientific Reports*, 2018, arXiv:1707.08542 [cond-mat.soft].
- [62] J. P. Hansen and I. McDonald, in *Theory of Simple Liquids with Applications to Soft Matter*, Academic Press, 2013.
- [63] V. Tudisca, M. Ricci, R. Angelini and B. Ruzicka, *RSC Advances*, 2012, **2**, 11111–11116.
- [64] H. Tanaka, S. Jabbari-Farouji, J. Meunier and D. Bonn, *Phys. Rev. E*, 2005, **71**, 021402–9.
- [65] B. Ruzicka, E. Zaccarelli, L. Zulian, R. Angelini, M. Sztucki, A. Moussaïd, T. Narayanan and F. Sciortino, *Nat. Mater.*, 2011, **10**, 56–60.
- [66] B. Ruzicka, L. Zulian and G. Ruocco, *Phys. Rev. Lett.*, 2004, **93**, 258301–4.

- [67] D. Saha, J. M. Yogesh and R. Bandyopadhyay, *Soft Matter*, 2014, **10**, 3292–3300.
- [68] B. Ruta, E. Pineda and Z. Evenson, *J. Phys.: Condens. Matt.*, 2017, **29**,.
- [69] Q. Li, X. Peng and G. B. McKenna, *Soft Matter*, 2017, **13**, 1396–1404.
- [70] S. Havlin and D. Ben-Avraham, *Advances in Physics*, 1987, **36**, 695–798.
- [71] I. M. Sokolov, *Soft Matter*, 2012, **8**, 9043–9052.
- [72] M. Palombo, A. Gabrielli, V. D. P. Servedio, G. Ruocco and S. Capuani, *Sci. Rep.*, 2013, **3**, 2631–7.
- [73] U. Balucani and M. Zoppi, *Dynamics of the Liquid State*, Clarendon Press; 1 edition, 1995, vol. 10.
- [74] C. Bennemann, J. Baschnagela and W. Paul, *Eur. Phys. J. B*, 1999, **10**, 323–334.
- [75] W. Götze, *Götze Complex Dynamics of Glass-Forming Liquids-A Mode-Coupling Theory*, Oxford University Press, USA, 2009.
- [76] C. Angell, *Proc. Natl. Acad. Sci. USA*, 1995, **92**, 6675–6682.
- [77] R. Casalini, *J. Chem. Phys.*, 2012, **137**, 204904–4.
- [78] S. Sengupta, F. Vasconcelos, F. Affouard and S. Sastry, *J. Chem. Phys.*, 2011, **135**, 194503–9.
- [79] Z. Shi, P. G. Debenedetti, F. H. Stillinger and P. Ginart, *J. Chem. Phys.*, 2011, **135**, 084153–9.
- [80] N. Gnan and E. Zaccarelli, *arXiv:1806.04788 [cond-mat.soft]*, 2018, 1–14.